ESTRATTO

NE-Vol. 15, Thermal Hydraulics of Advanced
Steam Generators and Heat Exchangers
ASME 1994

DATA ON CHF BY DRYOUT FOR PRESSURIZED WATER IN SMALL DIAMETER TUBES

Adriano M. Lezzi
Dipartimento di Ingegneria Meccanica
Università di Brescia
Brescia
Italy

Alfonso Niro
Dipartimento di Energetica
Politecnico di Milano
Milano
Italy

THERMAL HYDRAULICS OF ADVANCED STEAM GENERATORS AND HEAT EXCHANGERS

presented at
1994 International Mechanical Engineering Congress and Exposition
Chicago, Illinois
November 6–11, 1994

sponsored by
The Nuclear Engineering Division, ASME

edited by
Y. A. Hassan
Texas A&M University

D. S. Cassell
University of Tennessee

K. Okamoto
University of Tokyo

M. Cho
Foster Wheeler Energy Corporation

THE AMERICAN SOCIETY OF MECHANICAL ENGINEERS
UNITED ENGINEERING CENTER / 345 EAST 47TH STREET / NEW YORK, NEW YORK 10017

ISBN No. 0-7918-1422-X

Library of Congress Catalog Number 94-78990

NE-Vol. 15, Thermal Hydraulics of Advanced
Steam Generators and Heat Exchangers
ASME 1994

DATA ON CHF BY DRYOUT FOR PRESSURIZED WATER IN SMALL DIAMETER TUBES

Adriano M. Lezzi
Dipartimento di Ingegneria Meccanica
Università di Brescia
Brescia
Italy

Alfonso Niro
Dipartimento di Energetica
Politecnico di Milano
Milano
Italy

ABSTRACT

Experimental data on critical heat flux (CHF) in forced convection flow boiling in horizontal capillary tubes are presented. Results for two different diameters, $D = 0.5$ and 1 mm, are compared for a nominal length-to-diameter ratio equal to 1000. Data are for water at 30, 50, and 70 bar, mass flux ranging from 500 to 6600 kg/m^{2}s, and inlet conditions between saturation and strong subcooling. In all cases the fluid quality at the tube exit is high and critical heat flux is reached through dryout. The experimental results are compared with extrapolations of the Katto-Ohno and the CISE correlations.

INTRODUCTION

Flow boiling in capillary tubes is recognized as a promising technique in heat transfer enhancement. For example, in compact heat exchangers, high power exchange per unit volume is usually achieved by means of extended surfaces with very large contact area. An alternative to finned tubes, however, as suggested by Echigo *et al.* (1992), is to use small diameter tubes to increase the contact area per unit volume. Flow boiling in capillary tubes has been investigated lately in relation to the high-performance cooling devices which are necessary for the development of some fusion reactor components (see, e.g., Celata, 1993, and Mishima *et al.*, 1993). It finds applications also in cooling of electronic power components: heat sinks made of a thin metal block containing small channels with diameter ranging from 0.1 to 1 mm, are currently under development and testing (Bowers and Mudawar, 1994).

In the literature, data on critical heat flux (CHF) for forced convection boiling in capillary tubes are scarce. Bergles (1963) investigated CHF in tubes with inner diameter as small as 0.6 mm and found that CHF is enhanced by decreasing the tube diameter. This behaviour has been confirmed by much recent work related to fusion reactor technology (Celata, 1993). These data are all obtained under conditions of subcooled or low quality flow boiling at CHF location, when the mechanism responsible for the critical condition is known as departure from nucleate boiling (DNB).

An entirely different mechanism is at work for high exit quality flows. The flow pattern is annular and CHF condition is caused by the drying out of the liquid film at the wall. Existing correlations for high quality CHF predict a slight increase of the critical heat flux with the decrease of the tube diameter for fixed length-to-diameter ratio. However, these correlations are valid for diameters greater than a few millimeters.

In this study, we present experimental results on CHF in flow boiling of water in long horizontal capillary tubes. Two different diameters are investigated, $D = 0.5$ and 1 mm, keeping the length-to-diameter ratio equal to 975, approximately. CHF data are for low and intermediate mass fluxes (between 500 and 6600 kg/m^{2}s); outlet pressure equal to 30, 50, and 70 bar; and subcooled inlet conditions varying from 0 up to 250 K. In all cases the fluid quality at the tube outlet is higher than 0.45 and critical heat flux is reached through dryout.

Results are compared with extrapolations of the correlations proposed by Katto and Ohno (1984), and by CISE (Bertoletti *et al.*, 1965). A satisfactory overall agreement of the data with the values predicted by the correlations seems to suggest that, at least for tube diameters down to 0.5 mm, the effect of diameter on CHF for water does not differ from that characteristic of larger diameters.

EXPERIMENTAL APPARATUS AND PROCEDURE

A schematic diagram of the experimental apparatus used in this study is shown in Fig. 1. Demineralized water is drawn from a tank by a volumetric pump with maximum volume flow rate of 11 dm^3/h. In order to reduce pressure oscillations, the pump is connected to a 0.3 dm^3, bladder-type accumulator, pressurized with nitrogen (residual pulsation < 1%).

The preheating section is a horizontal, 3.5 m long, 1 mm i.d., 0.5 mm wall thickness, AISI 304 stainless steel tube heated uniformly by Joule effect using a 100 A, 2.5 kW, d.c., switch mode power supply. A pressure drop at the section exit provides that saturation conditions can be reached at the test section entrance with no boiling in the preheating section. The test section is a horizontal, straight AISI 304 stainless steel tube with smooth inner surface. Two different tubes are employed: one with inner diameter equal to 0.5 mm and wall thickness equal to 0.2 mm, the other with 1 mm i.d. and 0.25 mm wall thickness. The test section is heated uniformly by Joule effect using a 200 A, 5 kW, d.c. power supply. Copper clamps brazed at the two extremes provide the electric current to the tube and also its mechanical support. The electric power supplied to the test section is computed by multiplying the measured voltage drop across the heated tube length and the current flowing through the tube walls. The current is evaluated by measuring the voltage drop across a precision shunt resistor.

About 1 cm upstream of the downstream copper clamp of the test section, a K-type thermocouple is silver-brazed on the outside wall. This temperature reading (T_w) signals when critical heat flux is reached. The tube length L is defined as the heated length between the upstream copper clamp and the wall thermocouple.

The test section is mounted between two 4-way 1/8 in cross fittings. Each fitting is connected via 1/8 in piping to a strain-gauge absolute pressure transducer. The fitting provides access also for a 0.5 mm J-type thermocouple mounted with its junction at the centerline of the water flow. These measurements (p_{in}, p_{out}, T_{in}, T_{out}) allow to evaluate inlet water pressure and subcooling, and exit pressure. The distance between the wall thermocouple and the location where p_{out} and T_{out} are measured is about 4 cm.

Downstream of the test section, the flow passes first through the inner tube of a counterflow double-pipe condenser which cools it down to ambient temperature, and then through a pressure regulating valve which is operated manually.

The voltages across the test section and the shunt resistor, as well as the thermocouple voltages corresponding to T_{in}, T_{out}, T_w and the pressure transducer signals are read in a 5-second cycle by a data acquisition unit, and sent to an on-line PC for storage and visualization.

The experimental procedure consists of the following actions. First, the pump flow rate is preset and the exit valve is regulated to obtain the desired outlet pressure p_{out}. Then the power supplied to the preheating section is gradually increased until the desired operating value of T_{in} is reached. After thermal stabilization of the system, the experiment

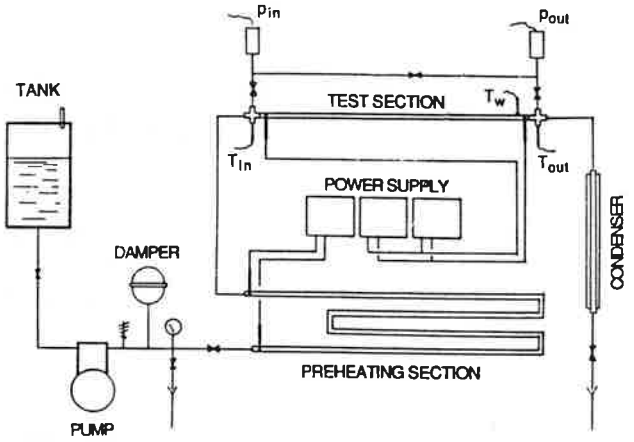

FIGURE 1. SCHEMATICS OF THE EXPERIMENTAL APPARATUS.

is conducted by increasing step by step the input power to the test section. As CHF conditions are approached, small adjustments of pressure and preheating power allow regulation of outlet pressure and inlet subcooling as desired. At any power step the reading of T_w varies very little as far as heat flux remains below below CHF, whereas above CHF T_w increases significantly with any further power increase, clearly indicating that CHF has been exceeded.

The data collected during an experimental run are post-processed in order to compute the average and the standard deviation of data recorded between two consecutive changes of the test section power. As power is increased the following events are observed. At first, T_w remains practically constant with a standard deviation smaller than 1 K. As CHF condition is approached, T_w exhibits fluctuations characterized by a standard deviation between 1 and 10 K. A 1 or 2 K increment of the average value of T_w is common at this stage. Eventually T_w begins to increase substantially at any power increment.

An average value of T_w 5 K larger than the practically constant pre-crisis value is adopted as a criterion for detecting the onset of CHF condition. Since the test section is not thermally insulated, the power determined in this way is corrected by subtracting the heat loss due to radiation and natural convection around the test channel, and to conduction through the copper clamps and the unheated entrance and exit lengths. The error made in calculating the heat losses is estimated to be within 10 W, which is equivalent to a relative error smaller than 1% in determining the actual power supplied to the fluid.

The mass flow rate G is measured by direct weighing of the water outflow over a period of time. The error is estimated to be within 2%. Temperatures are converted from thermocouple voltages with ASTM standard calibrations. The standard limits of error at typical operating temperatures are within ±2.2 K. The absolute error in pressure measurements are estimated to be within ±0.03 MPa.

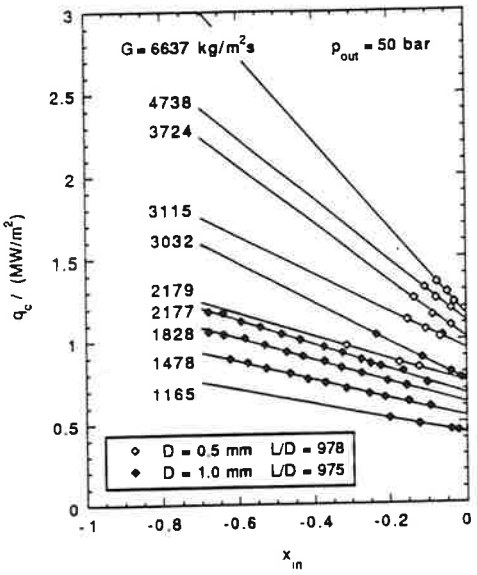

FIGURE 2. CHF DATA VERSUS INLET QUALITY.

RESULTS AND DISCUSSION

It is generally acknowledged that the critical heat flux is influenced mainly by five independent variables, namely the mass flux, the system pressure, the inlet subcooling, the tube inner diameter, and the tube heated length. In this study experimental CHF data are collected for two different inner diameters ($D = 0.5$ and 1 mm) and one fixed length-to-diameter ratio ($L/D = 978$ for $D = 0.5$ mm and $L/D = 975$ for $D = 1$ mm). Data are obtained for mass flux G between 500 and 6600 kg/m^{2}s ($G = 1300 - 6600$ kg/m^{2}s for $D = 0.5$ mm and $G = 500 - 3000$ kg/m^{2}s for $D = 1$ mm); for outlet pressure p_{out} approximately equal to 30, 50, and 70 bar with a ± 1 bar tolerance; and for inlet thermodynamic conditions ranging from saturation to strong subcooling, corresponding to inlet qualities $0 \geq x_{in} > -0.7$. The inlet quality is defined as $x_{in} = (h_{in} - h_f)/h_{fg}$ where the saturated liquid enthalpy h_f and the evaporation enthalpy h_{fg} are evaluated at inlet pressure p_{in}. The total number of data is 136: 44 for $D = 0.5$ and 92 for $D = 1$ mm.

In view of the moderate mass fluxes and high L/D ratio, the outlet thermodynamic quality at CHF condition is high ($x_{out} \geq 0.5$ for 96% of data). Under these conditions the flow is annular for most of the test section and critical heat flux is reached by dryout.

It is well known that the critical heat flux depends linearly on inlet subcooling. Following Katto (1985), the linear dependence is expressed as

$$q_c = q_{co}(1 - K x_{in}) \qquad (1)$$

where q_{co} is the so called basic CHF, i.e. the critical heat flux at zero inlet quality, and K is the inlet subcooling parameter. In Fig. 2 a representative sample of our CHF data is plotted versus x_{in} for several values of G. As is seen from the figure, the data correlate very well. This fact allows to obtain q_{co} and K by extrapolating at $x_{in} = 0$ each series of data characterized by the same values of D, L/D, G, and p_{out}. Extrapolated values are listed in Table 1 together with the corresponding mean values of G and p_{out}, and estimates of x_{out}. Missing K's refer to unreliable values.

TABLE 1. EXTRAPOLATED CHF VALUES AT ZERO INLET QUALITY.

G kg/m^{2}s	p_{out} bar	p_{in} bar	x_{out}	q_{co} MW/m^2	K
	$D = 0.5$ mm		$L = 489$ mm		
1351	29.8	34.1	0.937	0.554	1.076
2399	30.1	40.6	0.874	0.888	1.091
3027	30.2	44.8	0.804	1.004	1.493
2179	50.1	54.5	0.850	0.741	0.962
3115	49.9	60.2	0.778	0.943	1.216
3724	50.0	62.2	0.707	1.009	1.744
4738	50.0	65.5	0.629	1.111	1.681
6637	50.0	70.5	0.495	1.150	2.305
2848	70.0	74.7	0.582	0.604	1.766
4099	70.1	77.0	0.480	0.702	2.283
	$D = 1$ mm		$L = 975$ mm		
521	30.0	31.6	0.972	0.228	0.787
1228	29.0	36.2	0.887	0.478	-
1526	29.9	40.0	0.905	0.596	1.109
2685	30.1	48.9	0.741	0.809	1.294
782	50.3	51.8	0.979	0.315	1.009
1165	50.1	54.4	0.911	0.432	1.062
1478	50.2	56.3	0.892	0.532	1.074
1828	50.1	57.9	0.841	0.615	1.085
1882	49.9	59.0	0.842	0.631	1.107
2177	50.1	59.4	0.778	0.671	1.133
3032	50.0	63.7	0.645	0.750	1.598
560	69.0	69.7	0.914	0.195	1.208
692	69.3	70.3	0.886	0.233	1.193
896	70.0	71.8	0.846	0.286	1.198
1111	70.6	73.2	0.844	0.352	-

TABLE 2. CHF UNDER INLET THERMODYNAMIC CONDITIONS OF NEAR SATURATION.

G kg/m^{2}s	p_{out} bar	p_{in} bar	x_{out}	x_{in}	q_c MW/m^2
	$D = 1$ mm		$L = 975$ mm		
1765	30.0	42.7	0.905	-0.018	0.695
2708	29.9	48.4	0.719	-0.031	0.825
2945	30.2	49.7	0.686	-0.033	0.850
1870	50.5	58.8	0.834	0.000	0.621
2230	50.0	60.5	0.781	0.000	0.687
1421	71.0	73.8	0.712	-0.016	0.387
1470	70.5	74.5	0.742	0.000	0.407
1810	69.5	75.1	0.687	0.000	0.461

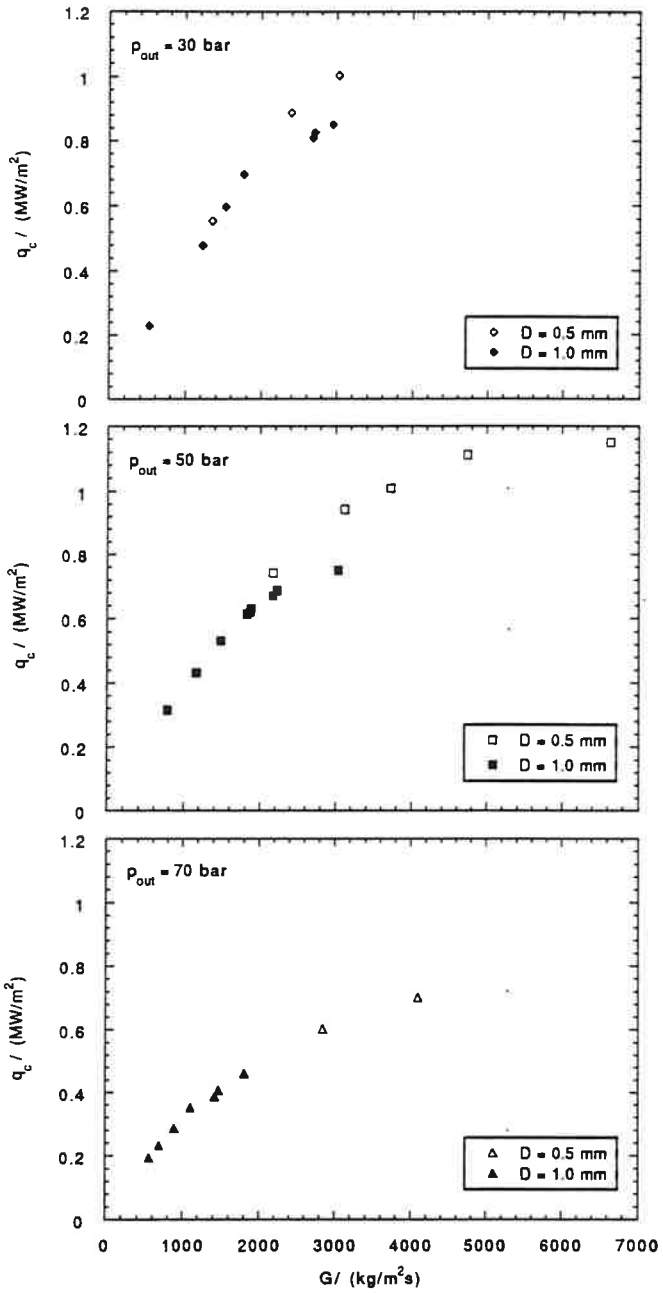

FIGURE 3. CHF DATA VERSUS MASS FLUX AT INLET CONDITIONS OF NEAR SATURATION.

Data in Table 1 allow an analysis of the influence of mass flux, pressure, and inner diameter on CHF, independently of inlet subcooling effects. In Fig. 3, the critical heat flux is plotted versus water mass flux for both inner diameters and fixed conditions of outlet pressure. Among the points plotted in Fig. 3 there are eight which do not appear in Table 1. These data are listed in Table 2 and correspond to experimental test runs with inlet conditions of near saturation, x_{in} being always greater than -0.033 (subcoolings between 0 and 11 K). They are shown in Fig. 3 because

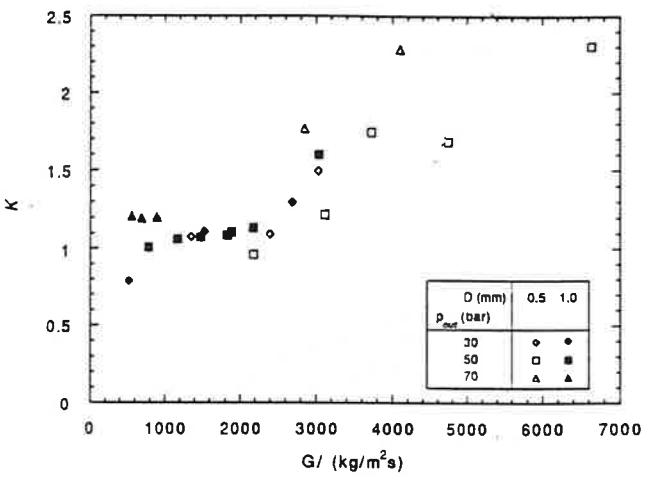

FIGURE 4. INLET SUBCOOLING PARAMETER VERSUS MASS FLUX.

they overestimate the corresponding q_{co} with a relative error smaller than 5% and they do not belong to any series used to obtain the q_{co} values in Table 1.

The data presented in this study show the same qualitative features of CHF data assessed for larger diameters. In particular, for fixed D, L/D, and p_{out}, CHF is an increasing function of mass flux. Instead, CHF decreases with pressure for fixed D, L/D, and G, as reported by Collier (1981) for the intermediate pressure range from about 30 to 100 bar.

Regarding the dependence on the diameter for fixed L/D ratio, G, and p_{out}, data at 30 and 50 bar suggest that CHF attains larger values at smaller diameters. With the necessary caution due to the small number of points available for comparison, it can be observed that the increment is significant at intermediate mass fluxes, but seems to be negligible at low values of G. Nothing can be said at $p_{out} = 70$ bar because in this case the data for different diameters extend over mass flux ranges that do not overlap.

The hypothesis of the existence of two distinct CHF trends at low and intermediate mass fluxes is reinforced by the behavior of the inlet subcooling parameter. As is shown in Fig. 4, K tends to stay approximately constant and slightly larger than one for G smaller than about 2500 kg/m^{2}s, whereas above this value K seems to increase rapidly with G. The data are not clear enough to draw any conclusion about the influence of pressure or diameter on K.

It is interesting to compare the CHF data from our experiments with estimates obtained from existing correlations valid for positive exit quality CHF. We have chosen the ones proposed by Katto and Ohno (1984), by CISE (Bertoletti *et al.*, 1965) and by Bowring (see Collier, 1981, pp. 265–267), even though our data lie beyond their original ranges of validity. The correlations differ substantially in kind. The Katto-Ohno correlation is semi-empirical, valid for an arbitrary fluid and based

TABLE 3. COMPARISON BETWEEN EXPERIMENTAL DATA AND EXTRAPOLATIONS OF CORRELATIONS.

	Katto-Ohno	CISE	Bowring
Mean $q_{c,calc}/q_{c,exp}$	1.11	0.87	1.35
RMS relative error	16.8%	15.2%	42.4%
Points in ±20% band	76.5%	83.8%	29.4%

on dimensionless groups. It was derived using an experimental data set covering mainly a diameter range from 3 to 11 mm, with only 3% of the data for diameters between 1 and 3 mm (Katto, 1980). The CISE correlation is empirical, valid for water in tubes with diameters between 7 and 25 mm. Here it has been chosen because it is extensively verified for CHF with annular flow pattern. The Bowring correlation is empirical, based on the hypothesis that q_c is determined by the local conditions at the tube exit irrespective of tube length. Although this hypothesis has been shown to have only approximate validity, the use of Bowring correlation is recommended by general references (Collier, 1981, and Rohsenow, 1985) for water in tubes with diameters between 2 and 45 mm.

Table 3 lists for each correlation the mean value of the ratio $q_{c,calc}/q_{c,exp}$ between predicted and experimental values; the RMS error; and the fraction of points which fall within the ±20% band.

Correlations are usually based on the assumption that the tube pressure drop is negligible and a single pressure value is ascribed to the system. Here p_{out} and $(h_{fg})_{out}$ are used for pressure and evaporation enthalpy, respectively. In this study, however, pressure losses are significant (up to 15 bar), therefore we have also made calculations using p_{in} and $(h_{lg})_{in}$. The relative differences between the two choices are within a few percent and indicate that pressure losses play only a secondary effect on CHF prediction.

Table 3 indicates a satisfactory agreement between our data and extrapolations of Katto-Ohno and CISE correlations which seem to supply an upper and lower bound for CHF in long, capillary tubes. In view of this agreement, it is useful to analyze $q_{c,calc}/q_{c,exp}$ in terms of its dependence on G, p_{out}, and D. In Fig. 5, for example, the ratio between computed and experimental CHF is plotted versus G for the Katto-Ohno correlation. The comparison is restricted to the data reported in Tables 1 and 2, that is to points characterized by inlet thermodynamic conditions of near saturation. For fixed p_{out} and D, the difference between experimental and predicted values of CHF increases with G. The increment is small at low G (all the points fall within the ±10% band with the exception of three points at $p_{out} = 70$ bar and $D = 1$ mm), but it is substantial at intermediate mass fluxes. About the dependence on pressure, the Katto-Ohno correlation seems to predict with the same error data at 30 and 50 bar, and with a larger error data with $p_{out} = 70$ bar, other conditions being equal.

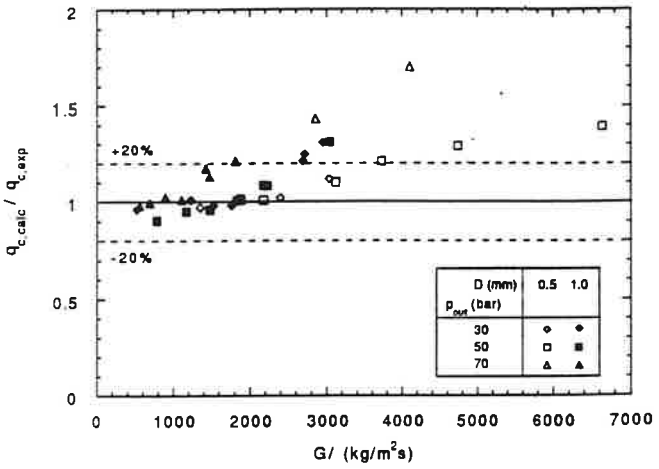

FIGURE 5. COMPARISON WITH EXTRAPOLATION OF THE KATTO-OHNO CORRELATION.

Finally, $q_{c,calc}/q_{c,exp}$ is higher for $D = 1$ mm than for $D = 0.5$ mm at intermediate G, where it is possible a comparison between different diameters.

A deeper insight can be obtained by plotting our data using dimensionless variables. The Katto-Ohno correlation describes the behavior of CHF for zero inlet subcooling in terms of three variables,

$$\frac{q_{co}}{Gh_{fg}} = f\left(\frac{\rho_g}{\rho_f}, \frac{\sigma\rho_f}{G^2L}, \frac{L}{D}\right). \qquad (2)$$

The function f takes on different forms associated with three distinct regimes, i.e., the L-regime which occurs for low mass flux, the N-regime for high mass flux, and the intermediate H-regime. In the L- and H-regime, the flow pattern at the tube exit is spray annular, whereas in the N-regime the flow is bubbly. Moreover, Katto (1981) has suggested that CHF might be due to liquid film dryout on the heated wall in the L-regime, and to liquid film breakdown in the H-regime, whereas it appears closely related to DNB in the N-regime.

In Fig. 6, the boiling number q_c/Gh_{fg} is plotted versus the dimensionless parameter $\sigma\rho_f/G^2L$ for near saturation data. Solid lines represent the CHF behavior as predicted by the Katto-Ohno correlation. It is noteworthy that the density ratio ρ_g/ρ_f, which depends on pressure only, appears explicitly in the correlation in the H-regime, but not in the L-regime. Therefore, curves corresponding to different pressures coincide in the L-regime and separate only after transition to H-regime. As $\sigma\rho_f/G^2L$ decreases, transition from L- to H-regime occurs first at $p_{out} = 30$ bar, then at 50 bar, and eventually at 70 bar.

Regarding to the experimental data, the following observations can be made.

The length to diameter ratio L/D is practically the same for both $D = 0.5$ and 1 mm, so that, according to the Katto-Ohno correlation, points with the same p_{out} should lie on a single curve, irrespective of D. This feature is clearly shown in Fig. 6, expecially for data with $p_{out} = 30$ and

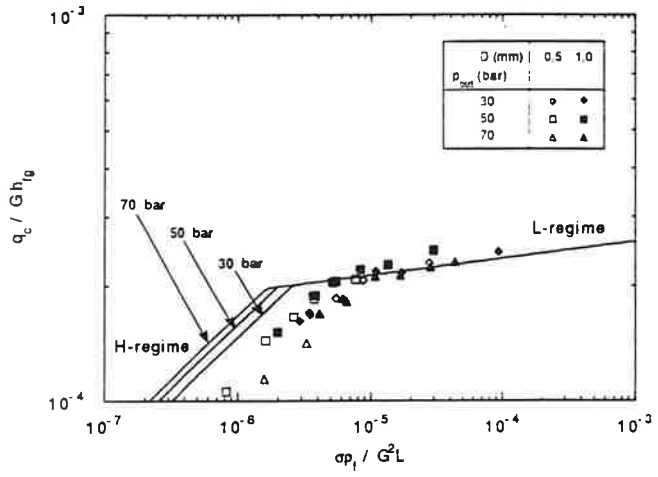

FIGURE 6. COMPARISON WITH EXTRAPOLATION OF THE KATTO-OHNO CORRELATION. BOILING NUMBER VERSUS $\sigma\rho_f/G^2L$.

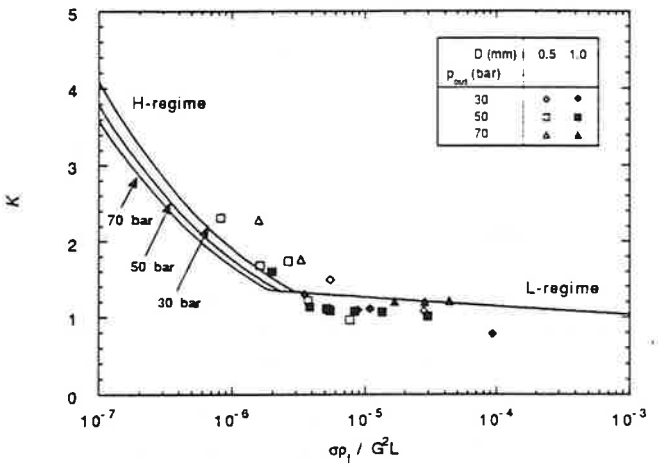

FIGURE 7. COMPARISON WITH EXTRAPOLATION OF THE KATTO-OHNO CORRELATION. INLET SUBCOOLING PARAMETER VERSUS $\sigma\rho_f/G^2L$.

50 bar, providing an evidence of self-consistency of the data presented in this study.

There is an overall qualitative agreement between data and predicted curves. The distribution of the experimental points confirm the existence of two distinct trends: at higher values of the parameter $\sigma\rho_f/G^2L$ (low G), the data fall rather close to the L-regime curve of the Katto-Ohno correlation and show a good quantitative agreement which is independent on p_{out} and D; at lower $\sigma\rho_f/G^2L$ (intermediate G), instead, there is an apparent dependence on p_{out} and the boiling number increases much more rapidly with $\sigma\rho_f/G^2L$. These features are characteristic of the H-regime and, indeed, the data points tend to distribute along lines parallel to the H-regime curves predicted by the correlation.

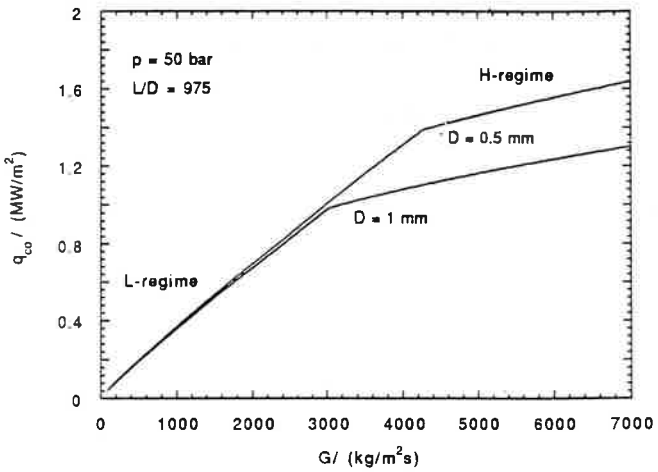

FIGURE 8. CHF BEHAVIOR AS PREDICTED BY THE KATTO-OHNO CORRELATION.

However, the transition between the two regimes occurs at larger values of $\sigma\rho_f/G^2L$ than those predicted and in wrong order with respect to pressure, as is evident for data with $p_{out} = 70$ bar. The existence of two distinct regimes in the range of parameters covered by our experimental data is confirmed also by a comparison between the values of the inlet subcooling parameter K in Table 1 and extrapolations of the Katto-Ohno correlation, as is shown in Fig. 7.

The discrepancy between our experimental data at intermediate G and the Katto-Ohno equation valid in the H-regime is most likely due to the high L/D value characteristic of our data, rather than to the use of very small diameter ducts. As observed by Katto (1985), the range of validity of the correlation in the H- and N-regime might be limited to $L/D < 600$, because of the very few data available in the literature above this threshold. Moreover, Figs. 6 and 7 do not display any different behavior between points for $D = 0.5$ mm and those for $D = 1$ mm.

Despite some numerical differences, we think that the Katto-Ohno correlation, even if extrapolated beyond its range of validity, retains the capacity of reflecting the physical mechanisms which determine CHF conditions. For example, the transition between L- and H-regime occurs around a critical value of the dimensionless parameter $\sigma\rho_f/G^2L$; if one varies D, keeping p_{out} and L/D constant, the corresponding value of G at transition is a decreasing function of D. With reference to Fig. 8, where q_{co} is plotted versus G for two values of D, pressure and L/D being equal, it can be observed what follows: *(a)* transition from L- to H- regime takes place at a lower G for $D = 1$ mm than for $D = 0.5$ mm; *(b)* when both tubes are in the L-regime differences in CHF are negligible; *(c)* over the G interval where $D = 1$ mm is in the H-regime and $D = 0.5$ mm is still in the L-regime, the difference between the two critical heat fluxes grows significantly because of the different dependence on G in the two regimes. This behavior is exactly the same exhibited by the experimental data and

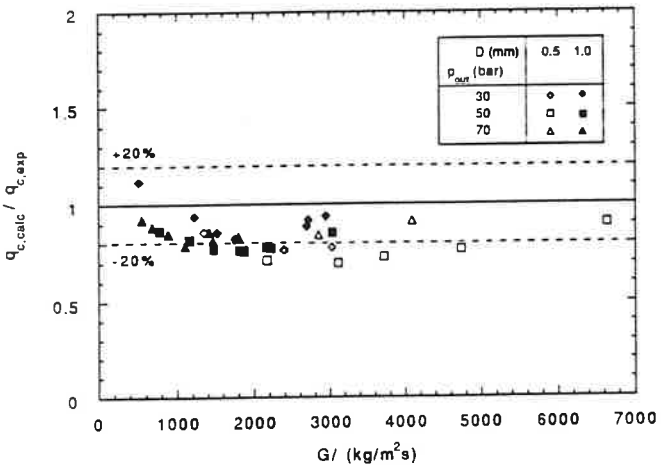

FIGURE 9. COMPARISON WITH EXTRAPOLATION OF THE CISE CORRELATION.

described commenting on Fig. 3.

In Fig. 9, the ratio $q_{c,calc}/q_{c,exp}$ is plotted versus G for the CISE correlation. As mentioned above, this correlation seems to give a lower bound for the critical heat flux since it underpredicts almost all data reported in this study. This property was already pointed out by the authors who developed the correlation (Bertoletti *et al.*, 1965, pp. 154 and 160). They noted that the tendency to underestimate CHF was enhanced when the correlation was used beyond the range of validity. Although the tubes used in this study have diameters much smaller than the recommended lower limit of validity (7 mm), it is important to remark that the CISE correlation gives a useful conservative estimate of CHF. As is seen in Fig. 9, the relative difference between experimental and predicted values does not appear to be influenced significantly by the mass flux, the outlet pressure, or the diameter.

We conclude considering the performance of the Bowring correlation. Table 3 indicates a poor agreement with the experimental data, which are largely overpredicted. It is noteworthy that the differences between experimental results and calculated values depend strongly on pressure. The RMS error, for example, is equal to 7% , 41% , and 68% for data corresponding to p_{out} = 30, 50, and 70 bar, respectively. The reason of this behavior is not clear at present.

CONCLUSIONS

In this work experimental data for CHF in long horizontal capillary tubes are presented. The data characterized by high exit quality, were collected for inner diameter equal to 0.5 and 1 mm, varying pressure, mass flux, and inlet subcooling. The length-to-diameter ratio was kept fixed.

Two distinct trends are recognized in the data and, upon comparison with the Katto-Ohno correlation, they are identified as corresponding to the L- and H-regime. There is a good quantitative agreement with predictions for data in the L-regime, but only a qualitative one in the H-regime. It is suggested that the difference might be due to the high length-to-diameter ratio, rather than to a small diameter effect. Under conditions of fixed outlet pressure and inlet subcooling, CHF attains a higher value as D decreases. This effect is significant only at intermediate values of G where transition from the L- to the H-regime has already occured.

Comparison with the CISE correlation shows that over the range of parameters covered in the experiment, this correlation provide a reliable conservative estimate for CHF.

We conclude that, for low and intermediate mass fluxes, high L/D ratios and tube diameters down to 0.5 mm, the effect of tube diameter on CHF does not seem to differ from that characteristic of larger diameters. However, work is still needed to confirm this conclusion. In particular, data for other values of L/D should be collected in order to verify if the quantitative differences between experimental data and prediction of the Katto-Ohno correlation tend to reduce for $L/D < 600$. In addition, since the flow pattern is annular for most of the test section, it should be intesting to check how the data compare with the prediction of CHF based on existing hydrodynamical models for annular flow.

ACKNOWLEDGEMENTS

The authors wish to thank Prof. G.P. Beretta for his valuable help and discussions during the preparation of this work.

Funding provided by MURST via 40% grants to the Università di Brescia and the Politecnico di Milano.

REFERENCES

Bergles, A.E., 1963, "Subcooled Burnout in Tubes of Small Diameter," ASME Paper, 63-WA-182.

Bertoletti, S., Gaspari, G.P., Lombardi, C., Peterlongo, G., Silvestri, M., and Tacconi, F.A., 1965, "Heat Transfer Crisis with Steam-Water Mixtures," *Energia Nucleare*, Vol. 12, pp. 121–172.

Bowers, M.B., and Mudawar, I., 1994, "High Flux Boiling in Low Flow Rate, Low Pressure Drop Mini-Channel and Micro-Channel Heat Sinks," *International Journal of Heat and Mass Transfer*, Vol. 37, pp. 321–332.

Celata, G.P., 1993 "Recent Achievements in the Thermal Hydraulics of High Heat Flux Components in Fusion Reactors," *Experimental Thermal and Fluid Science*, Vol. 7, pp. 177–192.

Collier, J.G., 1981, *Convective Boiling and Condensation*, 2nd ed., McGraw-Hill, New York, , pp. 248–274.

Echigo, R., Yoshida, H., Hanamura, K., and Mori, H., 1992, "Fine-Tube Heat Exchanger Woven with Threads," *International Journal of Heat and Mass Transfer*, Vol. 35, pp. 711–717.

Katto, Y., 1980, "General Features of CHF of Forced Convection Boiling in Uniformly Heated Vertical Tubes With Zero Inlet Subcooling," *International Journal of Heat and Mass Transfer*, Vol. 23, pp. 493–504.

Katto, Y., 1981, "On the Relation between Critical Heat Flux and Outlet Flow Pattern of Forced Convection Boiling in Uniformly Heated Vertical Tubes," *International Journal of Heat and Mass Transfer*, Vol. 24, pp. 541–544.

Katto, Y., 1985, "Critical Heat Flux," *Advances in Heat Transfer*, Vol. 17, pp. 1–64.

Katto, Y., and Ohno, H., 1984, "An Improved Version of the Generalized Correlation of Critical Heat Flux for the Forced Convective Boiling in Uniformly Heated Vertical Tubes," *International Journal of Heat and Mass Transfer*, Vol. 27, pp. 1641–1648.

Mishima, K., Nishihara, H., Kureta, M., and Tasaka, K. 1993, "Critical Heat Flux for Low Pressure Water in Small Diameter Tubes," *Proceedings, 6th International Topical Meeting on Nuclear Reactor Thermal Hydraulics*, Grenoble, Vol. 1, pp. 435–443.

Rohsenow, W.M., 1985, "Boiling," in *Handbook of Heat Transfer Fundamentals*, 2nd ed., W. M. Rohsenow, J. P. Hartnett and E. N. Ganic, eds., McGraw-Hill, New York, Chap. 12.